

# Crystal Structure and Magnetic Properties of $\text{Tb}_{11}\text{O}_{20}$

S. BARAN<sup>a</sup>, R. DURAJ<sup>b</sup>, A. HOSER<sup>c</sup>, B. PENC<sup>a</sup> AND A. SZYTUŁA<sup>a,\*</sup>

<sup>a</sup>M. Smoluchowski Institute of Physics, Jagiellonian University, W.S. Reymonta 4, 30-059 Kraków, Poland

<sup>b</sup>Institute of Physics, Technical University of Cracow, Podchorążych 1, 30-084 Kraków, Poland

<sup>c</sup>Helmholtz-Zentrum Berlin für Materialien and Energie GmbH, Hahn–Meitner-Platz 1, 14-109 Berlin, Germany

(Received September 14, 2012)

Magnetic and neutron diffraction data for  $\text{Tb}_{11}\text{O}_{20}$  compound are reported. This compound crystallizes in a triclinic crystal structure described by the space group  $P\bar{1}$  and is antiferromagnetic with the Néel temperature 5.1 K.

DOI: 10.12693/APhysPolA.123.98

PACS: 61.05.fm, 75.30.Kz, 75.40.Gb, 75.47.Lx, 75.50.Ee

## 1. Introduction

Binary terbium oxides form a large number of compounds showing different stoichiometry [1]. The essential compounds are  $\text{Tb}_2\text{O}_3$  and  $\text{TbO}_2$ . Both of them crystallize in a cubic crystal system, but they differ in their unit cells [2]. In the Tb–O system there also exists the non-stoichiometric  $\text{TbO}_{2-x}$  group of compounds with different crystal structure [3]. The paper [4] reports the crystal structures of new terbium oxides  $\text{Tb}_7\text{O}_{12}$  and  $\text{Tb}_{11}\text{O}_{20}$  as rhombohedral and triclinic ones, respectively.

Magnetic measurements indicate different magnetic ordering temperatures for different phases: 2.4 K ( $\text{Tb}_2\text{O}_3$ ), 3 K ( $\text{TbO}_2$ ) and 6 K ( $\text{TbO}_{1.823}$ ). For all these compounds the negative values of the paramagnetic Curie temperature suggest an antiferromagnetic order [5]. The specific heat data for  $\text{Tb}_2\text{O}_3$  and  $\text{Tb}_4\text{O}_7$  ( $\text{TbO}_{1.75}$ ) indicate the critical temperatures of magnetic order at 2.42 and 7.85 K, respectively [6].

In this work the X-ray and neutron diffraction as well as magnetic data for commercial sample of terbium oxide (purity 99.9%) by Johnson Malthey Company are reported. From these data the crystal structure parameters and magnetic properties are determined.

## 2. Experiment

Phase analysis was done by X-ray powder diffraction (XRD) at room temperature using a Panalytical X'PERT diffractometer with the  $\text{Cu } K_\alpha$  radiation.

The dc magnetic measurements were carried out using a commercial vibrating sample magnetometer (VSM) option of the Quantum Design PPMS. Three types of magnetic measurements were performed: cooling at low temperatures at zero magnetic field (ZFC) and at field (FC) equal to  $H = 50$  Oe (to determine the phase transition temperatures), then scanning from 1.9 K up to 300 K in a magnetic field of 1 kOe (to determine the value of the effective magnetic moment  $\mu_{\text{eff}}$  and the paramagnetic

Curie temperature  $\theta_p$ ) and finally measuring the magnetization curves up to 90 kOe at 1.9 K (to determine the value of the magnetic moment in the ordered state).

In order to determine precisely the temperature of the phase transition the ac magnetic susceptibility ( $\chi_{\text{ac}} = \chi' + i\chi''$ , where  $\chi'$  is the real and  $\chi''$  imaginary components) was measured versus frequency between 10 Hz and 10 kHz and in magnetic field amplitude  $H_{\text{ac}}$  equal to 5 Oe in the temperature range 2–10 K.

Powder diffraction patterns were collected using the E6 diffractometer installed at BERII reactor (Helmholtz-Zentrum Berlin) within the temperature range 1.6 and 300 K with incident neutron wavelengths equal to 2.447 Å. The X-ray and neutron diffraction data were analyzed using the Rietveld-type program Fullprof [7].

## 3. Results

Figure 1 shows the XRD pattern measured at room temperature. In this pattern the strong intensity Bragg reflections corresponding to the cubic crystal structure (space group  $Fm\bar{3}m$ ) are similar to those observed in  $\text{TbO}_2$  [8]. In this structure the Tb atoms occupy 4(a) site: 0, 0, 0 while O atoms 8(c) site: 1/4, 1/4, 1/4. However, the strong widening of the main peaks and the existence of additional small intensity ones indicate a lower symmetry. The best fit of the experimental data was obtained for the model of  $\text{Tb}_{11}\text{O}_{20}$  ( $\text{TbO}_{1.818}$ ) structure reported in Ref. [4]. This model is also verified by neutron diffraction data (see below).

The results of the dc magnetic measurements are shown in Fig. 2. Temperature dependence of magnetic susceptibilities gives the maximum at 4 K for ZFC curve and 3.4 K for FC curve. The values of  $\chi$  are higher for FC and for both the curves there is a quick decrease near 5 K. At 8.5 K the additional small intensity maximum is observed. Above 50 K the reciprocal magnetic susceptibility obeys the Curie–Weiss law with the paramagnetic Curie temperature  $-22.5$  K and effective magnetic moment equal to  $8.95 \mu_B$ . This value is between these for  $\text{Tb}^{3+}$  ( $9.72 \mu_B$ ) and  $\text{Tb}^{4+}$  ( $7.94 \mu_B$ ) and suggests the existence of both types of ions in the investigated compound. The negative values of the paramagnetic Curie

\*corresponding author; e-mail: andrzej.sztyula@uj.edu.pl

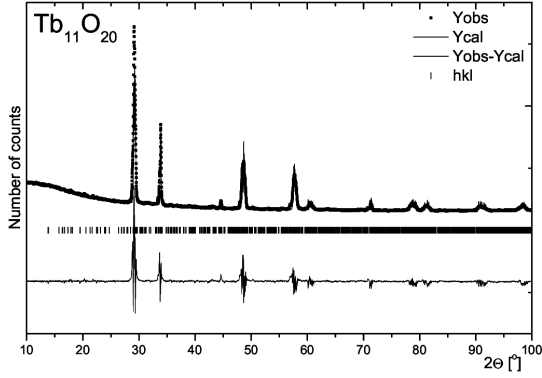


Fig. 1. The observed (dots) and calculated (solid line) X-ray diffraction patterns of terbium  $Tb_{11}O_{20}$  oxide measured at room temperature. The positions of Bragg reflections are marked as bars.

temperature indicate that the antiferromagnetic interactions are dominant. The magnetization curve measured at  $T = 1.9$  K is not saturated at  $H = 90$  kOe and it gives the average Tb moment equal to  $3.6 \mu_B$ .

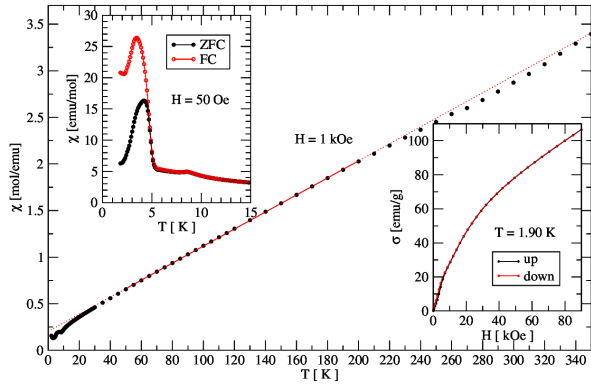


Fig. 2. Temperature dependence of the reciprocal magnetic susceptibility measured at 1 kOe for  $Tb_{11}O_{20}$ . The insets show: the upper one — temperature dependence of the magnetic susceptibilities: ZFC (lower curve) and FC (upper curve) and the lower one — magnetization curve up to 90 kOe at  $T = 1.9$  K.

Temperature dependence of the ac magnetic susceptibility  $\chi'$  and  $\chi''$  has a broad strong maximum at 4.5 K. The values of  $\chi'$  and  $\chi''$  in the region of the broad peaks (particularly  $\chi''$ ) strongly depend on frequency (see Fig. 3). Also the  $T_{max}$  corresponding to the maximum in  $\chi''(T)$  increases from 4.0 K for  $f = 10$  Hz to 4.3 K for  $f = 10$  kHz. All curves decrease to zero at  $T = 5.1$  K. In  $\chi'(T)$  an additional small maximum is observed at 8.5 K.

Neutron diffraction patterns measured at 1.6 and 11.8 K are shown in Fig. 4. Numerical analysis of the nuclear peak intensities is in a good agreement with the crystal structure of  $Tb_{11}O_{20}$ . In this low symmetry triclinic structure (space group  $P\bar{1}$ ) the Tb atoms occupy

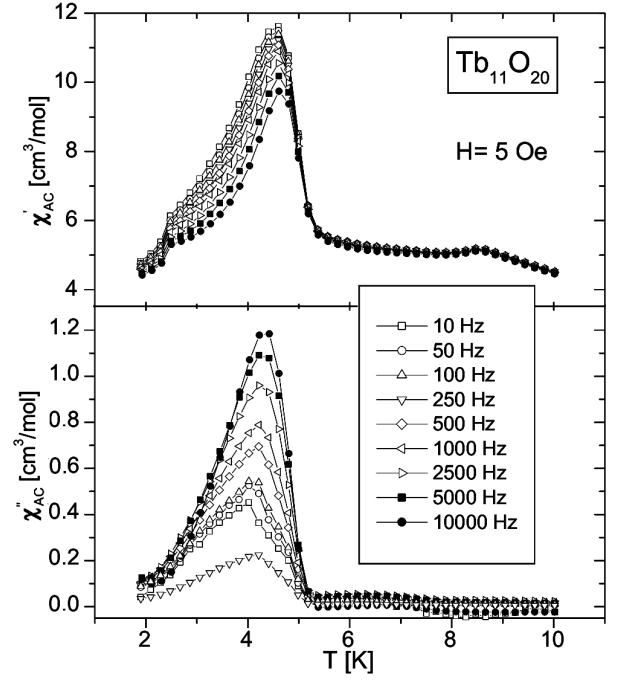


Fig. 3. Temperature dependence of the real  $\chi'$  and imaginary  $\chi''$  part of the ac magnetic susceptibility in the function of the frequency between 10 Hz and 10 kHz.

six different Wyckoff positions. Our data were analyzed using the positional atom parameters taken from Ref. [4].

TABLE

Crystal structure parameters for  $Tb_{11}O_{20}$  from neutron diffraction at 1.6 and 11.8 K and X-ray diffraction data at room temperature. These data are compared with those from Ref. [4].

$T$ [K]	1.6	11.8	300	[4]
$a$ [Å]	6.493(6)	6.494(2)	6.4893(2)	6.4878(4)
$b$ [Å]	6.514(6)	6.514(1)	6.5058(2)	6.50992(4)
$c$ [Å]	9.845(11)	9.838(3)	9.8364(3)	9.8298(6)
$\alpha$ [deg]	96.15(15)	96.11(4)	95.905(2)	95.881(1)
$\beta$ [deg]	99.36(12)	99.34(4)	99.292(2)	99.019(2)
$\gamma$ [deg]	100.01(9)	100.00(3)	99.919(2)	99.966(1)
$V$ [Å <sup>3</sup> ]	401.4(1.2)	401.2(3)	400.69(4)	406.68(7)

The determined lattice parameters  $a$ ,  $b$ ,  $c$  and angles  $\alpha$ ,  $\beta$ , and  $\gamma$  at different temperatures are listed in Table. Data obtained at room temperature are in a good agreement with those reported in Ref. [4]. In the region  $15^\circ$ – $40^\circ$  a broad maximum is observed in pattern collected at 11.8 K (see Fig. 4). With the decrease of temperature a group of small intensity Bragg reflections arises within mentioned above angle region. This fact indicates that Tb magnetic moments order and probably form a modulated structure at low temperatures. A large number of small intensity overlapping reflections of magnetic origin made impossible to determine magnetic structure.

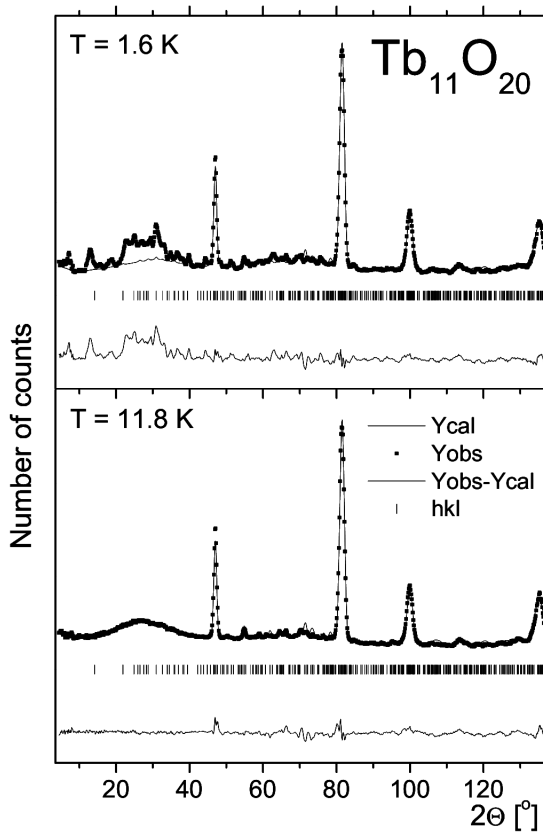


Fig. 4. Neutron diffraction patterns of  $\text{Tb}_{11}\text{O}_{20}$  measured at 1.6 and 11.8 K. The squares represent experimental points. The solid lines are: the calculated profile for crystal structure model (as described in the text) and the difference between the observed and calculated intensity (the bottom of each diagram). The vertical bars indicate the positions of Bragg peaks. In the pattern collected at  $T = 1.6$  K the angle region below  $2\theta = 45^\circ$  was excluded from refinement.

#### 4. Summary

The magnetic as well as X-ray and neutron powder diffraction data, reported in this work, indicate that terbium oxide  $\text{Tb}_{11}\text{O}_{20}$  ( $\text{TbO}_{1.818}$ ) order antiferromagnetically below 4.5 K. The compound has a complex crystal structure described by the triclinic space group  $P\bar{1}$ . The Tb magnetic moments form probably a modulated magnetic order at low temperatures.

The comparison of the Néel temperatures for different terbium oxides indicates the maximum of 7.85 K observed

for  $\text{Tb}_4\text{O}_7$  in which a coexistence of  $\text{Tb}^{3+}$  and  $\text{Tb}^{4+}$  ions was found. In  $\text{Tb}_{11}\text{O}_{20}$  also a mixture of  $\text{Tb}^{3+}$  and  $\text{Tb}^{4+}$  ions was determined leading to higher value of the Néel temperature. The lower Néel temperatures equal to 3 and 2.42 K were observed for  $\text{TbO}_2$  and  $\text{Tb}_2\text{O}_3$ , respectively. In these compounds only the  $\text{Tb}^{4+}$  ions in  $\text{TbO}_2$  or  $\text{Tb}^{3+}$  in  $\text{Tb}_2\text{O}_3$  were found. This result indicates that the exchange interaction between ions with different valence causes the increase of the Néel temperature. Similar effect was observed in manganites.

#### Acknowledgments

The research was carried out with the equipment purchased thanks to the financial support of the European Regional Development Fund in the framework of the Polish Innovation Economy Operational Program (contract no. POIG.02.01.00-12-023/08).

This research project has been supported by the European Commission under the 7th Framework Programme through the “Research Infrastructure” action of the “Capacities” Programme, NMI3-II grant number 283883. Kind hospitality and financial support extended for two of us (S.B. and A.S.) by Berlin Neutron Scattering Centre, Helmholtz-Zentrum-Berlin is gratefully acknowledged.

#### References

- [1] G. Adachi, N. Imanaka, *Chem. Rev.* **98**, 1479 (1998).
- [2] D.A. Burnham, L. Eyring, J. Kordis, *J. Phys. Chem.* **72**, 4424 (1968).
- [3] N.C. Baenziger, H.A. Eick, H.S. Schuldt, L. Eyring, *J. Am. Chem. Soc.* **83**, 2219 (1961).
- [4] J. Zhang, R.B. von Dreele, L. Eyring, *J. Solid State Chem.* **104**, 21 (1993).
- [5] J.B. MacChensey, H.J. Williams, R.C. Sherwood, J.F. Potter, *J. Appl. Phys.* **17**, 1435 (1966).
- [6] R.W. Hill, *J. Phys. C, Solid State Phys.* **19**, 673 (1986).
- [7] J. Rodriguez-Carvajal, *Physica B* **192**, 55 (1993).
- [8] J.B. MacChensey, H.J. Williams, R.C. Sherwood, J.F. Potter, *J. Chem. Phys.* **44**, 596 (1966).